# RTN in $Ge_xSe_{1-x}$ OTS Selector Devices

Zheng Chai[a], Weidong Zhang[a], Robin Degraeve[b], Jian Fu Zhang[a], John Marsland[a], Andrea Fantini[b], Daniele Garbin[b], Sergiu Clima[b], Ludovic Goux[b], Gouri Sankar Kar[b]

[a] Department of Electronics & Electrical Eng., Liverpool John Moores University, Liverpool L3 3AF, UK
[b] IMEC, Kapeldreef 75, B-3001 Leuven, Belgium

## Abstract

Random telegraph noise (RTN) signals in $Ge_xSe_{1-x}$ ovonic threshold switching (OTS) selector have been analyzed in this work, both before and after the first-fire (FF) operation and at on- and off-states. It is observed that RTN appears after the FF, and its absolute amplitude at the off-state is small and negligible in comparison with the RTN signals in RRAM devices. At the on-state, large RTN signals are observed, which can either partially or fully block the conduction path, supporting that a conductive filament is formed or activated by FF and then modulated during switching. Statistical analysis reveals that the relative RTN amplitude at on-state in $Ge_xSe_{1-x}$ OTS selector is smaller than or equivalent to those in RRAM devices.

**Keywords** – RRAM, random telegraph noise, OTS, selector, defects, filament
Email address: w.zhang@ljmu.ac.uk

## 1. Introduction

Resistive-switching random-access memory (RRAM) is considered a promising candidate among the emerging memory technologies [1-2]. However, the memory operation, the reliability and the maximum size of RRAM crossbar array are limited by the parasitic sneak paths, which are induced by the large leakage current flowing through the unselected RRAM devices [1-2]. To suppress the sneak paths, the one-selector-one-RRAM (1S1R) structure has been proposed [3-6]. The ovonic threshold switching (OTS) selector, which is based on a field-induced volatile switching mechanism, has been demonstrated by Ovshinsky in chalcogenide materials [1]. These materials have gained increasing interest from researchers for their high on-state current and high non-linearity (and hence low leakage current), which are required for the implementation of large memory arrays. Among the studied OTS materials, $Ge_xSe_{1-x}$ selector has become a strong contender because of its class-leading on-state current, high half-bias nonlinearity, fast switching, suitable voltage range and excellent endurance [4-6].

RTN is the fluctuation between discrete current levels in semiconductor devices, generally caused by trapping and de-trapping of charge carriers in defects. RTN has become a critical issue in nanoscale memory devices where the impact of a single defect becomes significant, as it could reduce the memory window and cause read errors [7-8]. RTN can also be a useful tool in exploring the defect behaviour from a microscopic perspective [7-8]. Impact of RTN has been analysed in various RRAM devices [7-9], but has not been reported in OTS selectors. In this work, RTN amplitude in $Ge_xSe_{1-x}$ OTS selector devices is analysed at different operation conditions, and its impact and correlation with switching mechanism are evaluated.

## 2. Device description and test setup

Amorphous $Ge_xSe_{1-x}$ films are prepared by room temperature physical vapor deposition (PVD). TiN/GeSe/ TiN selector devices were integrated in a 300 nm process flow, using a pillar (TiN) bottom electrode, which defines the device size down to 50 nm. A $Ge_xSe_{1-x}$ chalcogenide film thickness from 20 nm down to 5 nm was achieved and passivated with a low-temperature BEOL process scheme. The device structure and TEM are shown in Fig.1. The FF and switching were carried out by using a triangle pulse sweep with the Keysight semiconductor analyser B1500A and the I-V during the switching were recorded. RTN was measured either at the off-state, or at the on-state immediately following the switching. Typical I-V signals are shown in Fig.2. The device size being measured in this paper is 65 nm and the GeSe thickness is 10 nm. The OTS is connected to a 13 kΩ series resistor.

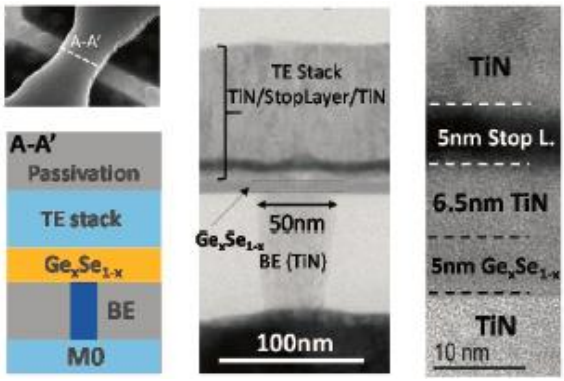


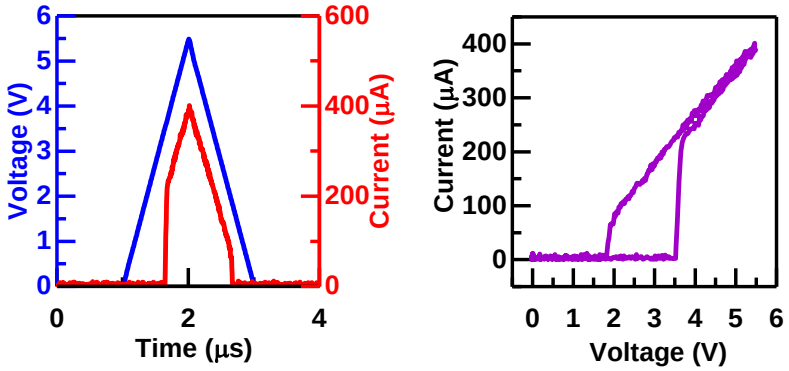


Fig.1 Device structure and TEM of GeSe-based OTS selector device. Fig.2: (a) Triangle voltage pulse and the measured current against time during the first-fire, and (b) its I-V plot. The OTS is in series with a 13kΩ resistor.

### 3. Results and discussion

To initiate the switching in the OTS devices, a first-fire (FF) operation is required in the first cycle, which has a switching voltage, $V_{FF}$, higher than the threshold voltage, $V_{th}$, in subsequent switching cycles. After the FF, the leakage current in the low voltage region (-1V, 1V) is increased by 1~2 orders, as shown in Fig.3. The cause of this increase will be investigated below.

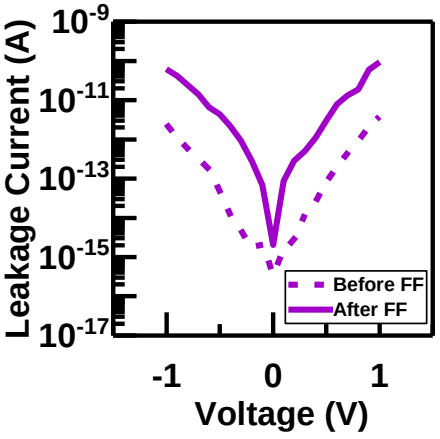


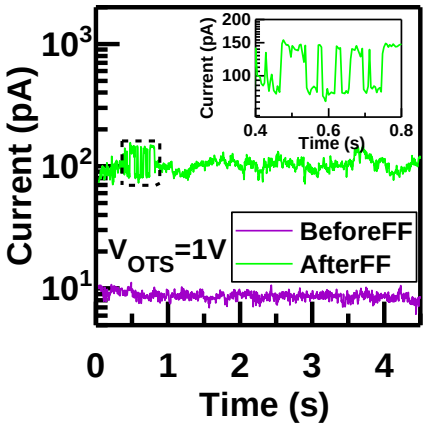


Fig.3: Leakage current measured at low bias before and after first fire. Fig.4: RTN signal measured at 1V before and after FF at off-state.

The RTN measured at off-state before and after the FF are compared in Fig.4. RTN starts to appear after the FF, indicating that the impact of defect trapping and de-trapping on current conduction becomes larger, in agreement with the observation in RRAM at off-state after the forming, where a filamentary percolation path is formed [7-8]. The RTN amplitude observed at off-state in OTS is in general less than 0.1 nA, much smaller than those observed in RRAM devices, and hence have limited impact on memory window.

RTN in RRAM devices can be measured after SET or RESET operations separately, thanks to its non-volatile nature. For the volatile OTS selector, however, the on-state RTN must be measured immediately after switching-on without any gap in between. Fig. 5 shows the waveform used for measuring the RTN after the device being switched on. Two types of RTN signal have been observed: RTN causing partial fluctuation similar to the off-state RTN, and RTN causing oscillation between the on- and off-state.

The two types of RTN indicate that the conduction path can be either partially or fully blocked, respectively, as shown in Fig.6. It should be noted that the RTN which fully blocks the conduction path can only be observed at lower biases close to the hold voltage ($V_{hold}$) at which the OTS selector is to be switched off. Therefore, in practical 1S1R RRAM array, it is essential to make sure that the selector is working under a high enough bias to avoid this on-off oscillation. In contrast, the RTN that partially blocks the conduction path can be observed at all bias conditions. The above observations confirm that the percolation conduction path does not exist in fresh devices, and it is induced by the FF, which also causes the increase of leakage current after FF in Fig.3. These results provide support to filament-type switching in OTS, as a single trapping and de-trapping event in a critical defect can switch on and off the entire conduction path, which must be in the form of a conductive filament.

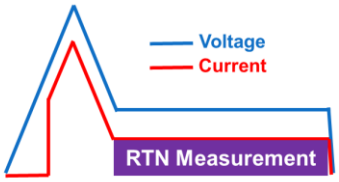


Fig.5: Waveform to measure on-state RTN. A constant bias following immediately the switching triangle pulse to measure the RTN before the OTS is switched off.

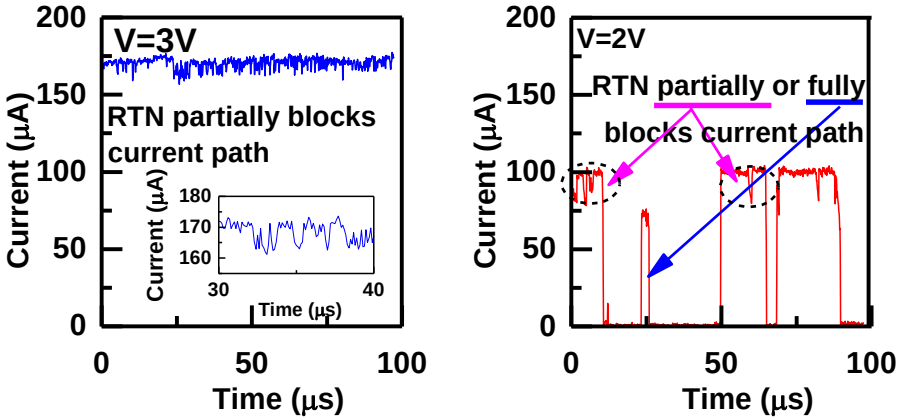


Fig.6: On-state RTN (a) at higher bias showing RTN that only partially blocks the current path, and (b) at lower bias showing RTN that both partially and fully blacks the current path.

Since the OTS selector allows the access to the RRAM device in the 1S1R structure only when it is at the on-state, it is important to analyse its on-state RTN amplitude distribution statistically and compare it with that of the RRAM device, and excessive RTN amplitude from the OTS selector may cause read-out error in the RRAM array. The relative RTN amplitude (ΔI/I) at on-state is observed to follow a lognormal distribution, as shown in Fig.7, similar to those observed in both the filamentary and non-filamentary RRAM devices [7-9]. It becomes smaller at higher bias and larger operation current, indicating the smaller impact of a single trap on the overall conduction when the filament becomes stronger. This is confirmed by the reduction of the averaged RTN amplitude at higher biases, as shown in Fig. 8. RTN amplitude at the on-state in OTS is found smaller than or equivalent to those observed in the filamentary and non-filamentary RRAM devices, as shown in Fig. 9. Furthermore, it is observed that temperature has little impact on the RTN amplitude in OTS, as shown in Fig. 10, demonstrating a good thermal stability regarding the RTN amplitude in the OTS selector.

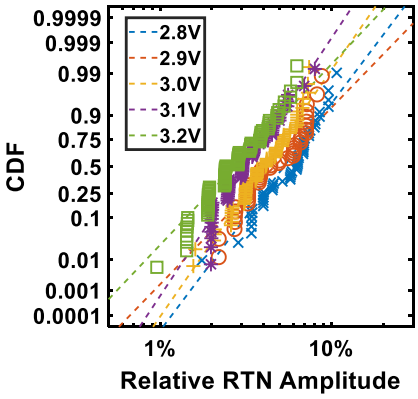


Fig.7 Amplitude of on-state partial RTN measured at different biases, which follow the lognormal distribution.

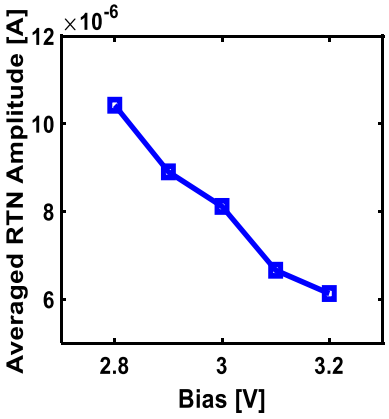


Fig.8: Averaged relative RTN amplitudes in OTS selector against the measurement bias.

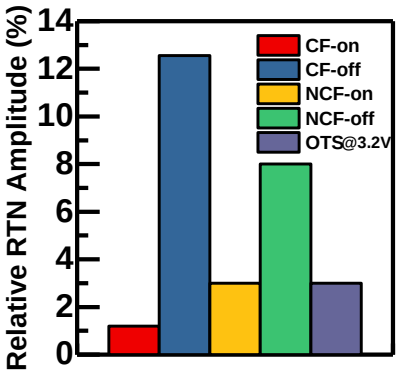


Fig.9: Comparison of relative RTN amplitude in filamentary RRAM (CF), non-filamentary RRAM (NCF) and OTS selector.

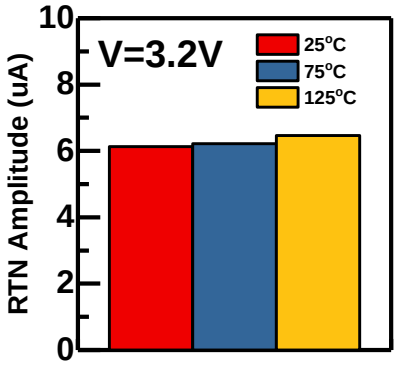


Fig.10: Absolute RTN amplitude at 25ºC, 75ºC and 125ºC showing good thermal stability. (Measured at 3.2V).

## 4. Conclusion

RTN signals in $Ge_xSe_{1-x}$ OTS selectors have been analysed in this work. It is observed that RTN signals appear after the FF operation but with very small amplitude at the off-state. Larger RTN signals that partially or fully block the conduction path are observed at on-state. These results support that a conductive filament has been formed during FF and is modulated during the switching. RTN amplitude at on-state in OTS is smaller than or equivalent to those in RRAM devices, showing promising potential in 1S1R applications.

**Acknowledgements**

The authors are grateful for the kind support of their colleagues in LJMU and IMEC. This work was supported by the EPSRC of UK (Grant nos.: EP/M006727/1 & EP/S000259/1).

**References**

[1] S.R. Ovshinsky, Reversible Electrical Switching Phenomena in Disordered Structures, Phy. Rev. Lett., 21 (1968) 1450. DOI: https://doi.org/10.1103/PhysRevLett.21.1450

[2] G. W. Burr, R. S. Shenoy, K. Virwani, P. Narayanan, A. Padilla, B. K. Hwang, Access devices for 3D crosspoint memory, J. Vac. Sci. Technol. B, 32 (2014) 40802-1-23 DOI: https://doi.org/10.1116/1.4889999

[3] L. Zhang, B. Govoreanu, A Redolfi, D. Crotti, H. Hody, V. Paraschiv, S. Cosemans, C. Adelmann, T. Witters, S. Clima, Y.Y. Chen, P. Hendrickx, D. Wouters, G. Groeseneken, M. Jurczak, High-drive current (>1MA/cm$^2$) and highly nonlinear (>10$^3$) TiN/amorphous-Silicon/TiN scalable bidirectional selector with excellent reliability and its variability impact on the 1S1R array performance, IEDM (2014). DOI: 10.1109/IEDM.2014.7047000

[4] B. Govoreanu, G.L. Donadio, K. Opsomer, W. Devulder, V.V. Afanas'ev, T. Witters, S. Clima, N.S. Avasarala, A. Redolfi, S. Kundu, O. Richard, D. Tsvetanova, G. Pourtois, C. Detavemier, L. Goux, G.S. Kar, Thermally stable integrated Se-based OTS selectors with >20 MA/cm2 current drive, >3.10$^3$ half-bias nonlinearity, tunable threshold voltage and excellent endurance, VLSI (2017). DOI: 10.23919/VLSIT.2017.7998207

[5] S. Clima, B. Govoreanu, K. Opsomer, A. Velea, N.S. Avasarala, W. Devulder, I. Shlyakhov, G.L. Donadio, T. Witters, S. Kundu, L. Goux, V. Afanasiev, G.S. Kar and G. Pourtois, Atomistic investigation of the electronic structure, thermal properties and conduction defects in Ge-rich GexSe1−x materials for selector applications, IEDM (2017). DOI: 10.1109/IEDM.2017.8268323

[6] N.S. Avasarala, G.L. Donadio, T. Witters, K. Opsomer, B. Govoreanu, A. Fantini, S. Clima, H. Oh, S. Kundu, W. Devulder, M. H. van der Veen, J. Van Houdt, M. Heyns, L. Goux, G. S. Kar, Half-threshold bias $I_{off}$ reduction down to nA range of thermally and electrically stable high-performance integrated OTS selector, obtained by Se enrichment and N-doping of thin GeSe layers, VLSI (2018). DOI: 10.1109/VLSIT.2018.8510680

[7] Z. Chai, J. Ma, W. Zhang, B. Govoreanu, E. Simoen, J.F. Zhang, Z. Ji, R. Gao, G. Groeseneken, M. Jurczak, RTN-based defect tracking technique: Experimentally probing the spatial and energy profile of the critical filament region and its correlation with $HfO_2$ RRAM switching operation and failure mechanism, VLSI (2016). DOI: 10.1109/VLSIT.2016.7573402

[8] J. Ma, Z. Chai, W. Zhang, B. Govoreanu, J.F. Zhang, Z. Ji, B. Benbakhti, G. Groeseneken, M. Jurczak, Identify the critical regions and switching/failure mechanisms in non-filamentary RRAM (a-VMCO) by RTN and CVS techniques for memory window improvement, IEDM (2016). DOI: 10.1109/IEDM.2016.7838466

[9] Z. Chai, P. Freitas, W. Zhang, F. Hatem, J.F. Zhang, J. Marsland, B. Govoreanu, L. Goux, G.S. Kar, Impact of RTN on Pattern Recognition Accuracy of RRAM-Based Synaptic Neural Network, IEEE Electron Device Lett. 39 (2018) 1652-1655 DOI: 10.1109/LED.2018.2869072